Fiber-Optic Biological/Chemical Sensing System Based on Degradable Hydrogel

Xiudong Wu, Hewei Liu, Xiaodong Wang, and Hongrui Jiang, *Fellow, IEEE*

***Abstract*— To improve the sensitivity and shorten the testing time of hydrogel-based bio-toxin sensors, we introduce an optical fiber Fabry–Perot interferometer (FPI) to detect the changes in the optical properties induced by the reactions between the target agent and the hydrogel. The concept is demonstrated by a polyacrylamide hydrogel filled into a cavity of an optical fiber FPI with a length of 150 μm. Dithiothreitol (DTT) solutions with different concentrations were used as target agent. The degradation of the hydrogel by the DTT solution leads to a long and indistinct change in optical properties, which is difficult to be observed by conventional microscopy methods, but which can be detected by measuring the unique shifting process of the interfering spectrum caused by the hydrogel cleavage in the FPI cavity. Compared to our previous hydrogel-based sensor based on the microscopy observation, the sensitivity of the optic fiber FPI is improved by 2000 times, and the testing time is shortened from hundreds of hours to a few hours. Our approach opens up an avenue for highly sensitive, high-speed in-field detection of bio-toxins in live samples.**

***Index Terms*— Bio-toxin detection, hydrogel sensor, fiber optics, microfluidics, Fabry–Perot interferometer.**

I. Introduction

THE detection of biological agents, especially bio-toxins, plays a crucial role in a broad range of applications related to biodenfense, environmental monitoring, food safety and public health [1], [2]. A large variety of detection schemes based on different principles have been developed, such as mouse lethality assay [3], enzyme-linked chemiluminescence assay [4]–[8], electrochemiluminescence [9], immune/real-time-polymerase chain reaction (PCR) [10], [11], cell culture assay [12], [13], surface plasmon resonance (SPR) [3], [14], and mass-spectrometry [15]. Despite their high sensitivity, these methods generally require time-consuming sample preparation or long incubation time, need high-cost, complicated instrument and skilled personnel, and are generally not suitable for in-field testing [14]. In addition, some of these methods, such as mass-spectrometry, cannot distinguish between active and inactive bio-toxins [15]. However, swift in-field testing is often of utmost importance in biodefense [16]. Therefore, there is enormous demand for a low-cost, easy-to-use, fast screening tool that allows for rapid in-field detection of active bio-toxins with high sensitivity and specificity.

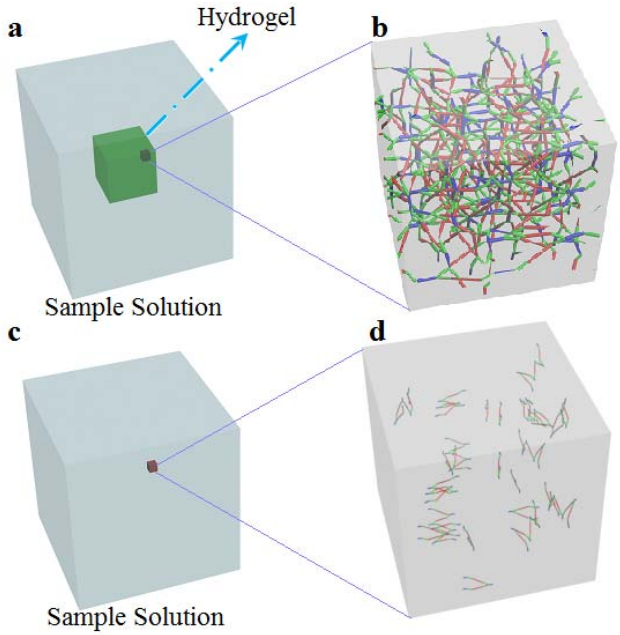

Fig. 1. Schematic diagram of the cleavage of the hydrogel. (a, b) The initial structure of the hydrogel before cleavage. (c, d) The structure of the hydrogel after cleavage.

Sridharamurthy *et al.* [17] previously reported on an autonomous sensing mechanism based on a polyacrylamide (PAAm) hydrogel. In this method, a crosslinker crosslinks water-soluble acrylamide chains to water insoluble network hydrogel (Fig. 1a, b). The crosslinker can be cleaved by a specific agent, and the hydrogel thus degrades and becomes water-soluble after the cleavage, revealing the presence of the toxin in the sample (Fig. 1c, d). Various biological agents could be detected utilizing different crosslinkers. This approach exploits the intrinsic protease activity of the corresponding enzyme and thereby leverages the inherent amplification function associated with the target enzyme. Hence, the potential sensitivity and specificity of this method

Manuscript received September 8, 2017; revised October 24, 2017; accepted October 26, 2017. Date of publication November 8, 2017; date of current version December 7, 2017. This work was supported by H. Jiang's Lynn H. Matthias and Vilas Distinguished Achievement Professorships. The associate editor coordinating the review of this paper and approving it for publication was Prof. Sang-Seok Lee. *(Corresponding author: Hongrui Jiang.)*

X. Wu, H. Liu, and X. Wang are with the Department of Electrical and Computer Engineering, University of Wisconsin–Madison, Madison, WI 53706 USA.

H. Jiang is with the Department of Electrical and Computer Engineering, the Department of Biomedical Engineering, the Department of Materials Science and Engineering, the Department of Ophthalmology and Visual Sciences, and the McPherson Eye Research Institute, University of Wisconsin–Madison, Madison, WI 53706 USA (e-mail: hongrui@engr.wisc.edu).

Digital Object Identifier 10.1109/JSEN.2017.2771398

could be extremely high. In addition, it is well suited for detecting bio-toxins, because many of them are proteases. For example, active botulinum neurotoxins could be detected with this method using a synaptosomal-associated protein (SNAP) 25-mer peptide as the crosslinker [18]–[20]. Although these works show the potential of low-cost, easy-to-use and in-field detection capability, a relatively large amount of toxin and long degradation process are needed to cause visible physical changes of the hydrogel. Consequently, the sensitivity and speed of detection is still much inferior to what this mechanism could offer.

To significantly improve the sensitivity and the speed of detection, we have adopted a fiber-optic method to detect refractive index (RI) change caused by the degradation of the hydrogel during the cleavage process [21], [22]. Sensors based on fiber optics, such as various fiber-based interferometers, have been widely studied in the detection of pH [23], glucose [24] and bacteria [25] owing to its small size, in-line structures and high sensitivity [26], [27]. Nevertheless, measurement of changes in the optical properties of hydrogels for toxin detection has yet been reported [28]. In this work, we present a PAAm hydrogel sensor based on an optic fiber Fabry Perot interferometer (FPI); its sensitivity is improved by 2000 times compared to our previous work [17]. As a demonstration, we applied dithiothreitol (DTT) solution to cleave a disulfide-crosslinked PAAm hydrogel, and monitored in real time in an optic fiber Fabry Perot interferometer (FPI) the unique spectral changes of the interference induced by the degradation of the PAAm hydrogel due to the DTT solution.

II. Detection Mechanism

In previous works utilizing the mechanism discussed above, the presence of the target agent could only be confirmed after the hydrogel was completely degraded, showing a clear and visible change in morphology. The degradation process in fact induces a continuous change of optical properties of the hydrogel, such as the RI [29]. Hence, monitoring such change in the RI throughout the degradation process could confirm the cleavage of the hydrogel at a very early stage, even at the onset, when there is still no distinguishable morphological change in the hydrogel. To demonstrate this concept, we used N, N' – bis(Acryloyl) crystamine as the crosslinker to closslink the PAAm hydrogel inside the cavity of the optic fiber FPI. DTT solutions were utilized to cleave the disulfide bond in the closslinker (see section II A), and thus change the optical property such as the RI of the hydrogel. As a result, the interference of light in the optic fiber FPI varied, showing shifts in the reflected spectrum obtained from an optical spectrum analyzer (OSA), which in turn was used to determine the degradation of the hydrogel (see section II B).

A. Degradation of Hydrogel by DTT Solution

Fig. 2 shows the chemical reaction of the cleavage of the hydrogel by DTT. Before degradation, the hydrogel is water-insoluble. DTT is a reducing agent that can break the disulfide bond, hence the crosslinker. All products of the reaction then become water-soluble. Therefore, the hydrogel can now be dissolved by water. Fig. 1 shows the schematic

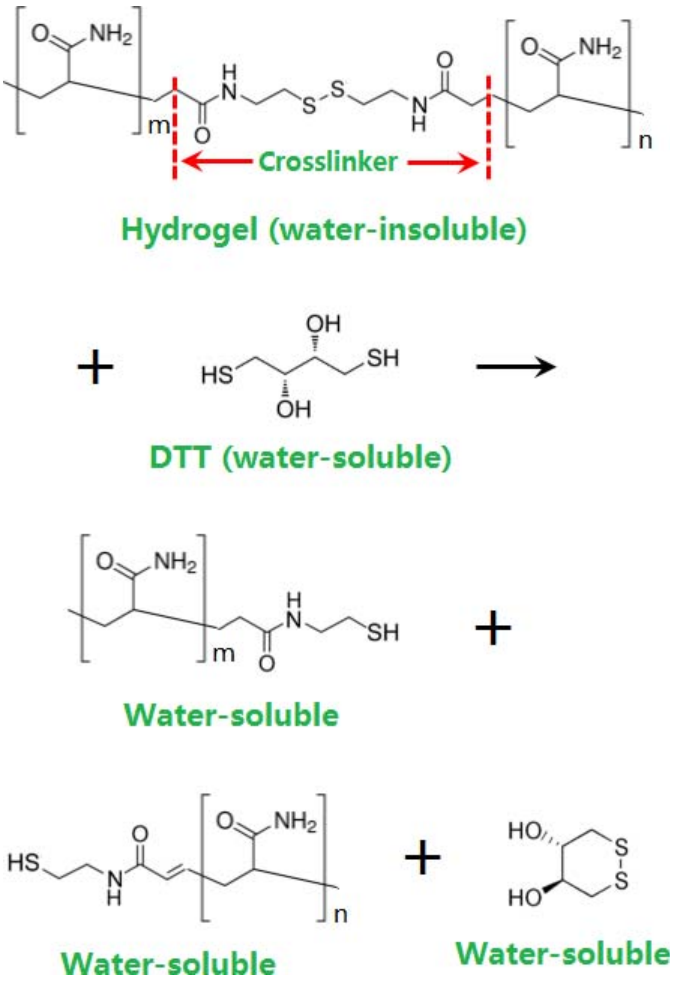

Fig. 2. The cleavage of the hydrogel. The disulfide bond in the hydrogel can be cleaved by the DTT. The hydrogel is initially water-insoluble, but all of the products after cleavage become water-soluble.

of the cleavage of the hydrogel by a target agent. Fig. 1(a, b) shows the status of the hydrogel before degradation, which is a gel, while Fig. 1(c, d) shows the status afterwards. In prior works [18]–[20], clearly visible morphology change before and after the degradation must be present to confirm the detection of the target agent, meaning that the cleavage reaction had to be almost finished. However, once the cleavage reaction starts, the RI of the hydrogel would change continuously until the end of the cleavage process, since the RIs of the reactants and the products are all different. Therefore, the target agent could be detected by monitoring the RI change of the hydrogel at the beginning of the cleavage reaction. This would significantly improve the sensitivity and detection speed compared with observing the morphology change of the hydrogel.

B. Detection of RI Change by Optic Fiber FPI

The structure of our device is schematically illustrated in Fig. 3 (a). A single-mode optic fiber is mounted in a chamber with one polished end facing a vertical glass slide, forming two end faces of the FPI cavity. A gap of around 150 μm between the fiber end and the glass slide is filled with closs-linked hydrogel. The reflected white light at the

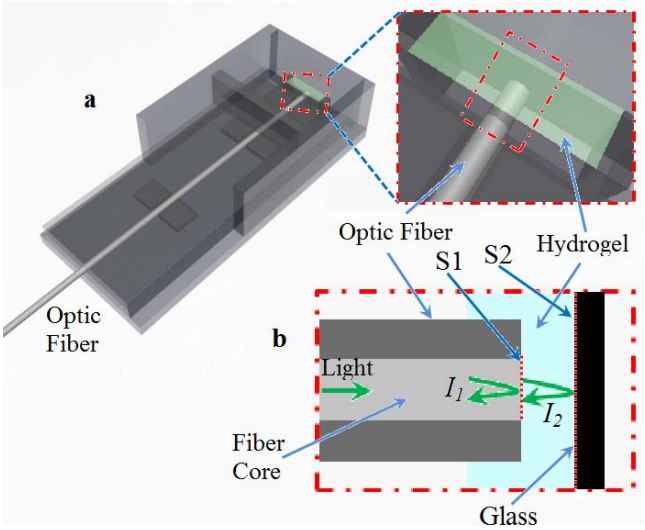

Fig. 3. (a) Schematic of an FPI device and the enlarged view of the FPI cavity. DTT cleaves the hydrogel (the green area) in the FPI cavity. As a result, the RI of the hydrogel would change. (b) Schematic illustration of the interfering process in the FPI cavity shown in (a). It shows the mechanism of the FPI. The RI change brings about the spectral shift for the FPI.

two end faces, S1 and S2, would interfere inside the core, as shown in Fig. 3 (b). Because the reflectivity at the end faces is low, multiple reflections in the cavity are negligible, and the interference of I_1 and I_2can thus be modeled by the following equation [30]:

$$I = I_1 + I_2 + 2\sqrt{I_1 I_2}\cos(\frac{4\pi n \times L}{\lambda} + \phi_0), \tag{1}$$

where I is the intensity of the interference, n the RI of the medium filling the cavity, L the length of the cavity, φ_0 the initial phase of the interference, and λ the optical wavelength in vacuum.

When the phase of the cosine term turns to an odd number of π, that is,

$$\frac{4\pi nL}{\lambda_v} + \phi_0 = (2m+1)\pi, \tag{2}$$

the interference intensity, I, reaches its minimum, which is the interference valley. Here, λ_v is the center wavelength of the interference valley. In our experiment, Lremained constant, and only the RI of hydrogel, n, induced the shifts in the interference valleys and peaks. After being exposed to the DTT solution, the network structure of hydrogel starts to be broken down and dissolved by water, causing a time dependent change of RI, n. According to Eq. (2), taking the derivative of n with respect to λ_v and assuming a constant L, we obtain:

$$\Delta\lambda_v = \lambda_v \times \frac{\Delta n}{n}, \tag{3}$$

which shows that the relative RI change of the hydrogel, Δn, is proportional to the interference valley shift, $\Delta\lambda_v$.

III. Experimental

A. Fabrication of Optic Fiber FPI

The FPI device was fabricated based on a fiber optics coupler (FOC; PLC-1X2, Fibertronics, Inc., FL, USA).

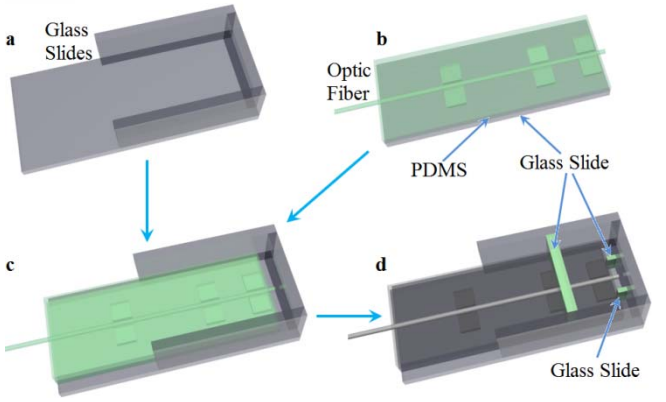

Fig. 4. The fabrication process of the FPI device. (a) Four glass slides are glued together. (b) The optic fiber is fixed on a glass slide with PDMS (in green). (c) The parts in (a) and (b) are combined using PDMS. (d) Three glass slides (in green) are glued to the device with PDMS.

The fabrication of the optic fiber FPI is shown in Fig. 4. First, four glass slides were glued together by ultra-violet (UV) glue after being exposed to UV light with an intensity of 25 mW/cm^2 for 1 min (Fig. 3(a)). Second, the end-section of the output fiber of the FOC was cut with an optic fiber cutter, followed by polishing using 5 different polishing films successively to smoothen its surface. Third, the prepared FOC was fixed on a glass slide by six rectangular solid polydimethylsiloxane (PDMS) blocks with the end face of the FOC positioned out of the side face by 2 mm. The sides of the six PDMS blocks were parallel to the long side of the glass slide, which is also the direction of the fiber. The structure was then applied liquid PDMS and placed on a hotplate at 90°C for 60 min to cure (Fig. 4(b)). Fourth, the components from step 1 and step 3 were combined using PDMS as adhesive (Fig. 4(c)). The process of combining the two was carefully performed under a microscope. The end of the fiber should be parallel to the opposite glass surface. It is important that the distance be around 100 μm between the end-section of the fiber and the corresponding opposite glass surface. If the distance is too large, the measured signal would be too weak; if the distance is too short, there would not be enough hydrogel between the two surfaces. Finally, the three glass slides (the green ones in Fig. 4(d)) were adhered to the device using PDMS (Fig. 4(d)). The distance between the two small glass slides is 3 mm, and the width of them is 1.5 mm. The large glass slide is 1.5 cm away from the opposing glass. The end section surface and the glass surface thus formed an FPI cavity (the green area in Fig. 3(a)). The liquid pre-gel solution would be injected into the cavity, and the four surrounding glass slides above the hydrogel (Fig. 3(a)) were to hold the liquid samples.

B. Synthesis of Hydrogel

In our experiment, the PAAm based pre-gel solution was photo-polymerized by UV light. The materials used for the pre-gel solution were acrylamine (AAm, Aldrich Chemicals), N, N' – bis(Acryloyl) crystamine (cross-linker, Aldrich Chemicals), 4-benzoy(benzyl) trimethyl-ammonium chloride (BP+, Aldrich Chemicals), N-methyl-diethanolamine

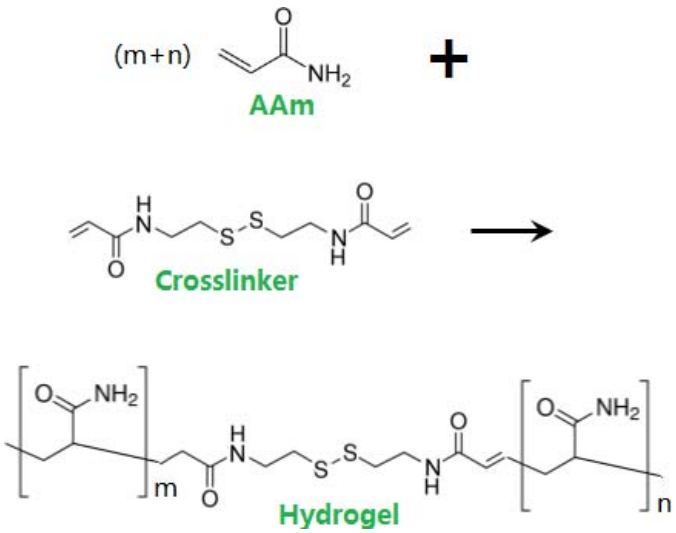

Fig. 5. The synthesis of the hydrogel.

(NMDA, Aldrich Chemicals), and DI water. These five materials were mixed in a ratio by weight (0.15: 0.00375: 0.02: 0.02: 1) to obtain 10 mL of pre-gel solution.

The 10 μL pre-gel solution was injected into the cavity (the green area in Fig. 3(a)), and then exposed to UV light with a dose of 18 mW/s for 180 s to be polymerized. In the pre-gel solution, the monomer, acrylamide (AAm), would combine into AAm long chains, which is soluble by water. At the same time, the crosslinker would link those AAm long chains to a networked structure, which would then become insoluble to water. The related chemical reaction is showed in Fig. 5. After the photo-polymerization, the hydrogel was flushed by ethanol (100%) for 5 min to eliminate unpolymerized pre-gel solution, and the whole device was subsequently baked on a hotplate at 50 °C for 5 min to remove the ethanol. Afterward, 1 mL of DI water was injected to soak and prep the hydrogel for 5 hrs before the water was removed. This process was used to further remove the unpolymerized pre-gel solution, and could also eliminate the effect of hydrogel swelling forces. At this point, the interference spectrum stabilized and the device was ready for testing.

C. Experimental Setup

Fig. 6 shows a photo and the schematic diagram of the FPI sensing system. In our experiment, we used an OSA (AQ6370d, Yokogawa, Japan) to detect the interference spectrum of the reflected light. The light source (PLC-1X2, Fibertronics, Inc., FL, USA) was built into the OSA, which delivered a wide-spectrum near-infrared light with the wavelength of between 1475 and 1485 nm. The resolution of the OSA was set at 0.5 nm, and each data was the result of averaging 5 measurements. One output of the FOC was connected to the built-in light source in the OSA. The other output of the FOC was connected to the input of the OSA for measurement. The input of the FOC was integrated into the FPI device during the fabrication, as shown in Fig. 6 (b). Throughout the testing, the FPI device was wrapped by a wet parafilm (Bemis Company Inc, WI, USA) to prevent the evaporation of the liquid in the FPI. The whole device was

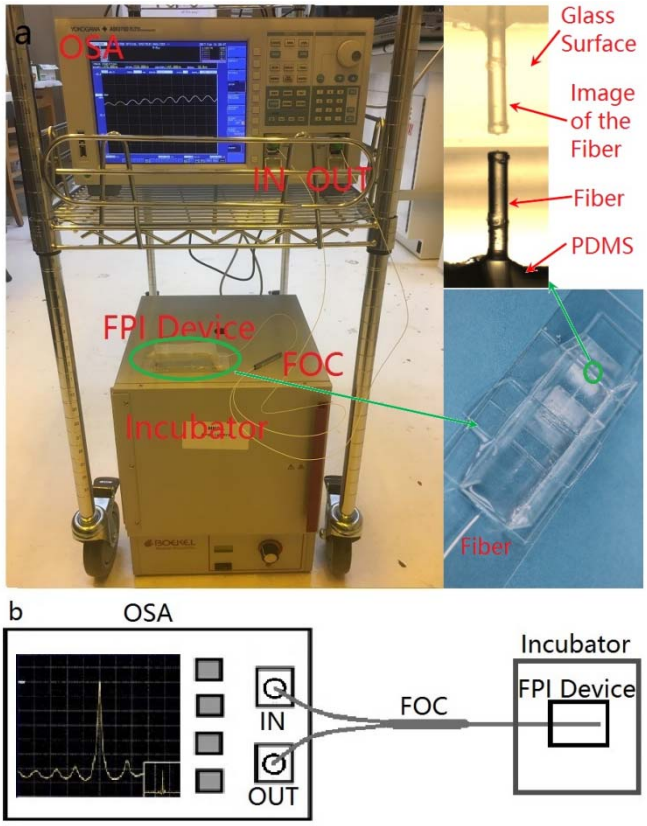

Fig. 6. Experimental setup of the FPI sensing system. (a) Photo of the experimental set up. (b) Schematic diagram of the experimental setup. The OSA serves as both the light source and the measurement apparatus. Two terminals of the FOC are connected to the light output and input of the OSA.

kept in an incubator at a temperature of 37±0.3 °C. To avoid the disturbance that might be induced by the vibrations of the instrument shelf, the incubator was placed on the lab floor, which is more stable, as shown in Fig. 6 (a).

IV. Results and Discussion

In a test, liquid samples were injected into the optic fiber FPI device with a syringe. The diffusion of the DTT from the liquid to the hydrogel and the resultant degradation of the hydrogel would disturb and shift the output spectrum of OSA. Before we tested with the DTT solutions, spectral shifts induced by the injection of DI water was first obtained as a reference data, representing the disturbances and the level of systematic errors in our testing system.

A. Spectral Shift Induced by DI Water

The hydrogel in the FPI cavity was previously immersed in DI water; therefore, adding new DI water would not change the RI and the texture of the hydrogel. Any variations in the spectrum obtained by the OSA were caused by the disturbances and systematic errors, which were recorded as reference data for the purpose of calibration. We injected 1 ml of DI water (37±0.3 °C, identical to the temperature of the hydrogel) into the optic fiber FPI cavity, and measured the spectra from the beginning (0 min) to 240 min after the injection. During the whole process, the FPI device was kept

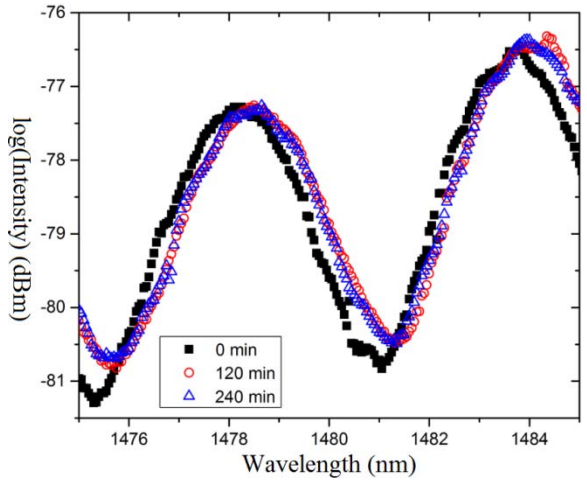

Fig. 7. The interfering spectrums acquired at 0 min, 120 min and 240 min after injection of DI water into the optic fiber FPI device.

in the incubator at a temperature of 37±0.3 °C. The spectra obtained at 0 min, 120 min and 240 min are shown in Fig. 7. It shows an initial slight red shift of about 0.5 nm after the DI water injection, and stabilization after 120 min. The red shift of the interfering spectrum with a rate of about 3 pm/min was mainly caused by the disturbance of liquid flow during the injection process of the DI water, and the systematic errors of the testing device. During this process, the maximum blue spectral shift rate was much less than 1 pm/min. If we keep the environment of and within the testing device identical, any spectral shifts beyond the shifting rate of 3 pm/min would indicate the change of optical properties of the hydrogel in the FPI cavity.

B. Spectral Shifts Induced by DTT Aqueous Solutions

The 1-ml DTT aqueous solutions with concentrations of 1 mM, 100 μM and 50 μM were utilized to demonstrate the capability of our optic fiber FPI sensor. The samples of the 1-mM and 100-μM solutions were kept in the incubator (37±0.3 °C) for 2 hours, to minimize the temperature difference between the DTT solution and the hydrogel. In order to investigate the effects of the temperature variations on the spectral shifting process, 20 °C DTT solution with a concentration of 50 μM was used for comparison. After the injection of the DTT solutions, the interfering spectra were acquired every 10 minutes. Fig. 8 shows the result of the spectral shifting process tested by the DTT solution with a concentration of 50 μM. We investigated the spectral shifting process by measuring the shifting distance of the spectral valley to the zero point at different times. The zero point is defined as the position of the spectral valley without DTT injection. Increase of the distance corresponds to the spectral shifts towards longer wavelength (red shift), while the decrease means the opposite (blue shift). The three groups of results obtained by the DTT solution with different concentrations are shown in Fig. 9.

In Fig. 9, the black squares show the test results with the 1-mM DTT solution. From 0 min to 40 min after the injection of the DTT solution, the spectrum shows a clear red shift

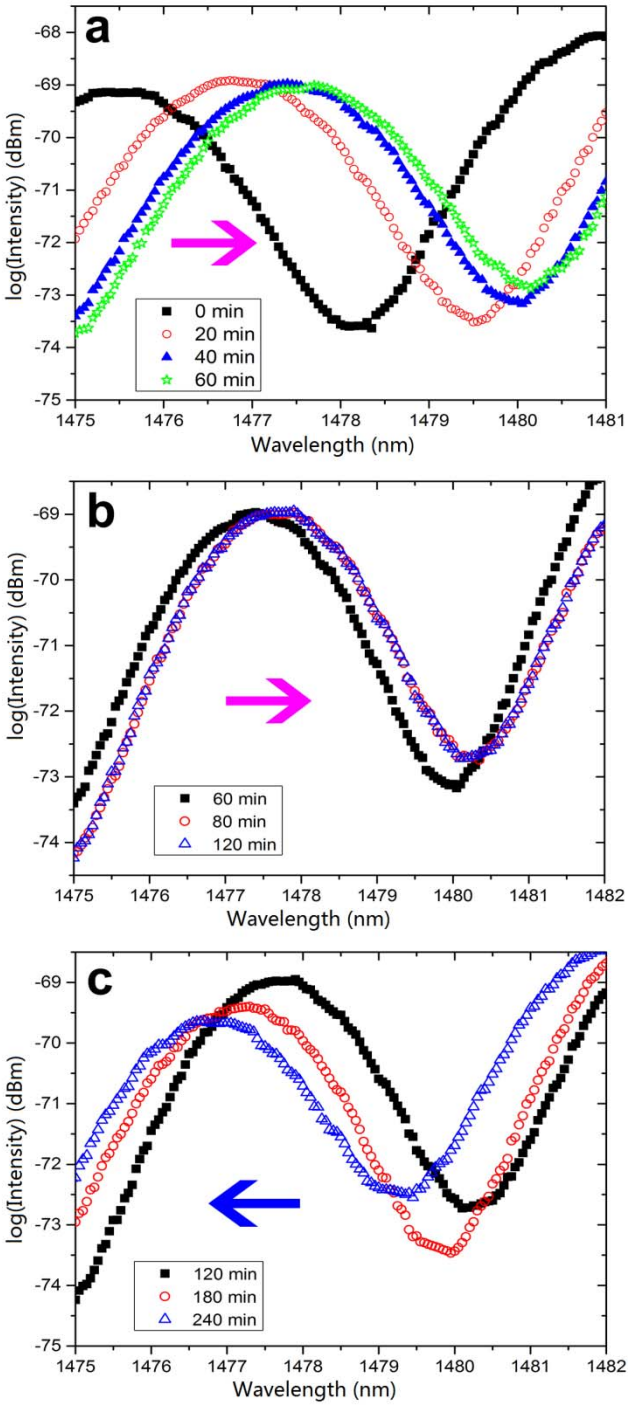

Fig. 8. The hydrogel tested with 50 μM DTT. The arrows show the shift directions. Before 120 mins, it is red shift, and the red shift rate decreases with time. After 120 mins, it becomes blue shift. The temperature at the beginning T(0) = 20 °C.

(the distance to the zero point increases) of about 2 nm. In the first 10 min, the shifting rate was much higher than the rest of time, which was about 150 pm/min, 50 times higher than the shifting rate of DI water. During the diffusion of the DTT into the hydrogel, the cleavage reaction decreased the refractive index, which shifted the spectrum to the shorter wavelengths (blue shift). The two processes competed with each other until the point of inflection came

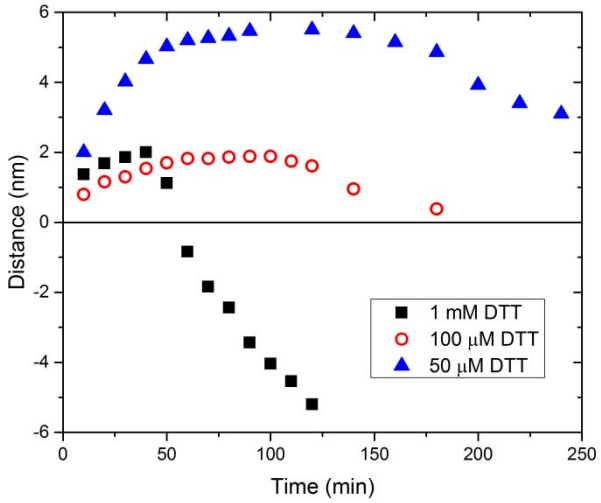

Fig. 9. The distance of the spectral shift after the injection of the DTT solutions with different concentrations. The zero point is the position of the spectral valley measured for the hydrogel without DTT solutions. The longer wavelength of the spectral valley compared with the zero point is defined as the positive distance.

at 40 min, when the blue shift started to dominate. From 40 min to 80 min, the spectrum shifted about 4 nm with a rate of about 100 pm/min. The blue spectral shift lasted much longer than the red spectral shift, indicating a long and slow degradation process of the hydrogel. From 80 min to 130 min, the spectrum continuously shifted to the short wavelength side with a decreased rate of about 20 pm/min. Because the rate of the blue spectral shift was still several times higher than the reference data obtained with DI water, it was mainly caused by the continuous change of the optical property of the hydrogel rather than disturbance or system errors. After 130 min, the blue spectral shift did not stop, but the shifting rate slowed down. Such long-time and continuous spectral shift with decreasing shifting rate was consistent with the chemical cleavage reaction process of the hydrogel. The concentration of the DTT decreased as the cleavage process proceeded, resulting in a slowing reaction.

Similar spectral shifts that combined red and blue shifts were also observed in the samples with DTT concentrations of 100 μM. For the 100-μM DTT solution (red circles in Fig. 9), the lower scattering effects of lights induced by lower concentration of DTT led to smaller initial red shift. Because the lower concentration of DTT induced more gentle cleavage process of the hydrogel, which prolonged the competing process between the initial red and blue spectral shift, the starting time of the blue shift was 100 min, which was much slower than that of 1-mM DTT solution (40 min).

In real-world applications, temperature control of the samples may not be available. In order to investigate the disturbance induced by the temperature change, we used a room temperature (20°C) DTT solution with a concentration of 50 μM for the testing. Once it was injected into the cavity, the temperature of the hydrogel was significantly decreased, leading to a red spectral shift from 0 to 60 min with a rate of 33 pm/min, as shown in Fig. 9 (blue triangles). The speed of red spectral shift declined from 60 min, and stopped at about 120 min, after which the blue shift began. The average rate of the blue shift was 10 pm/min (from 120 min to 240 min), which is much higher than that of the DI water, as shown in Fig. 7. Note that even though the concentration of DTT was reduced from 100 μM to 50 μM, the starting time of the blue spectral shift was almost the same. The initial red shift due to addition of the low-temperature sample might be related to the thermo-optic coefficient of PAAm hydrogel with a temperature decrease of about 17°C. The subsequent increase of the temperature in the incubator could also accelerate the blue spectral shift. This phenomenon will be helpful to shorten the stabilization period of the device and improve the testing speed.

C. Discussion

The shifting process of the interfering spectra indicates complicated optical processes in the FPI cavity after the DTT solution was injected. The fast initial red shift within tens of minutes after the sample injection refers to the drastic change of the temperature (demonstrated by the 50-μM DTT sample) or other optical properties (demonstrated by the 1-mM and 100-μM DTT samples), such as light scattering effects [31]. Meanwhile, the cleavage process of the hydrogel continuously decreases the RI of the hydrogel cavity by turning it from solid to liquid phase, and eventually pulls the interfering spectra back to the shorter wavelengths, starting a slow and long period of blue spectral shift. Such unique regulation of the spectral shift could exclude the non-target samples which only induce the changes of temperature or optical properties in the hydrogel cavity, but cannot cleave the hydrogel. For example, liquids with RI or temperature higher or lower than that of the hydrogel would induce fast red or blue spectral shifts, but the process would stop when the liquids are stabilized in the cavity, as demonstrated by the DI water results in Fig. 7, which only showed an initial red shift without long period of blue shift.

In addition, the spectral shifting rate in the hydrogel cavity reveals other information of the target samples. For example, the spectral shifting rates were different for various concentrations of the DTT solutions. For the DTT solution with lower concentration, both light scattering effects and hydrogel degradation process were weaker; therefore the rate of red and blue spectral shifts would be lower than the samples with higher concentrations, which postponed the starting time of the blue shift. Another factor that could significantly affect the shifting rate is the temperature difference between the sample and the hydrogel containing cavity. As demonstrated in Fig. 9, even though the concentration of the 50-μM DTT solution was lower than the other two samples, the decrease of 17 °C in temperature still increased the red spectral shift by several nanometers, and also accelerated the blue shift during subsequent warming process in the incubation chamber. Study of the temperature influences is important for the practical applications. In emergent situations, direct testing of samples without pre-heating treatments will save time and lives, but calibration of the temperature changes is needed for the accuracy of the testing. More importantly, we could prepare

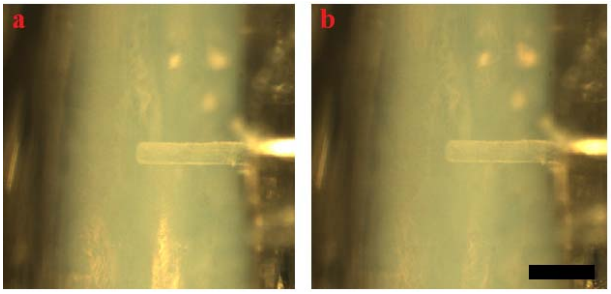

Fig. 10. Photos of the hydrogel at the beginning (a) and 4 hrs later (b) tested with 50 μM DTT. The light shadow is the hydrogel, and the small tube is the optic fiber. The scale bar is 350 μm.

the FPI sensors with higher temperature than the samples; the increase of the temperature in samples would shorten the testing time by accelerating the blue spectral shift to an earlier time.

The FPI sensor demonstrated in this work can significantly improve the sensitivity and efficiency of the detection. In our previous work [17], the concentration of the target agent needed to be at least 100 mM for a clear observation of the hydrogel degradation. The samples had to be continuously observed under a microscope for tens of hours. Besides, recognition of the morphological changes of the transparent hydrogel required highly-experienced operators. In this work, utilizing the FPI sensor, we can detect the DTT solution with a concentration down to 50 μM, which is 2000 times lower than the previous result. Instead of visually observing the phase change of the hydrogel, which needs tens of hours of wait until it is completely cleaved, the FPI sensor can detect the existence of the DTT or other bio-toxins by the inflection point of the red and blue spectral shifts within a few hours. Besides, recognition of the spectral shifts by the OSA is more accurate and reliable than the visual observations, which does not require experienced operators. Fig. 10 shows the photos of the hydrogel cavity after the 50-μM DTT solution was injected. The photos were taken under a microscope objective lens equipped with a high resolution CCD camera. We used the transmitted lighting mode to monitor any morphology changes inside the transparent hydrogel. 4 hours later, no visible morphological change of the hydrogel could yet be observed, as demonstrated in Fig. 10 (b). However, the interfering spectrum had already been shifted by several nanometers, which can be clearly detected by the OSA (the resolution of the OSA is 0.02 nm). The detection resolution of the FPI sensor is limited by the noise signals induced by the device. A stronger light source, smoother reflective surfaces between the hydrogel cavity and more uniform hydrogel can improve the detection resolution as well as the sensitivity of the device. Benefiting from the highly-sensitive interference optics, the detection of the degradation of the hydrogel, thus the presence of the cleaving agent, was accomplished within an hour. These results still have potential to be improved. For example, the thickness of the hydrogel applied in this experiment was 2 mm, which dramatically extended the diffusion and reaction time. If the hydrogel was patterned at the micro-scale, which could be achieved with well-established micro-lithography technologies, the detection speed as well as sensitivity of the device could be enhanced by several times.

V. Conclusion

We demonstrated an optic fiber FPI device that significantly improved the detection sensitivity and efficiency of biological and chemical sensors based on degradation of hydrogels. The hydrogels that we used in this work was PAAm hydrogel. The disulfide bond in the crosslinker of the PAAm hydrogel can be cleaved by a solution containing DTT, resulting in optical property changes in the hydrogel, even though they cannot be visually observed. By introducing the interfering optics, such changes can be detected as the evidence of hydrogel cleavage. In the experiment, we demonstrated a successful detection of DTT with concentration of 50 μM within 36 min. Compared to our previous work, the detection sensitivity was improved by 2000 times, and detection time was shortened from tens of hours to less than an hour. We tested our device with DTT solutions with different concentrations. The variations of the interfering spectra which combined a fast initial red shift followed by a slow and long period of blue shift were observed. Such unique spectral shifting process was related to complicated optical processes such as scattering, thermo-optic effects and hydrogel cleavage process. In future work, quantitative studies on the spectral shifts and their mechanisms are needed to provide more accurate measurement of the target agents. For example, the concentration of the samples could be estimated by analyzing the spectral shifting rates. Furthermore, we will explore to further improve the sensitivity and the detection speed by reducing the thickness of the hydrogel to quicken the liquid diffusion and hydrogel reaction process. The centimeter-sized FPI sensors are promising for high-precision, ultra-sensitive and fast in-field detection of biological and chemical agents.

Acknowledgment

The authors would like to thank Dr. Hao Bian and Liangzhi Lai for helpful discussions and technical assistance.

References

[1] M. A. Hamburg, "Bioterrorism: Responding to an emerging threat," *Trends Biotechnol.*, vol. 20, pp. 296–298, Jul. 2002.
[2] R. C. Spencer and N. F. Lightfoot, "Preparedness and response to bioterrorism," *J. Infection*, vol. 43, pp. 104–110, Aug. 2001.
[3] P. Cunniff, *Official Methods of Analysis of AOAC International*, 16th ed. Washington, DC, USA: AOAC International Inc., 1995, pp. 46–48.
[4] R. W. Phillips and D. Abbott, "High-throughput enzyme-linked immunoabsorbant assay (ELISA) electrochemiluminescent detection of botulinum toxins in foods for food safety and defence purposes," *Food Additives Contaminants*, vol. 25, pp. 1084–1088, Sep. 2008.
[5] B. Klaubert, N. Vujtovic-Ockenga, R. Wermter, K. Schad, and L. Meyer, "Determination of botulinum toxins after peptic sample pre-treatment by multidimensional nanoscale liquid chromatography and nano-electrospray ion-trap mass spectrometry," *J. Chromatogr. B*, vol. 877, pp. 1084–1092, Apr. 2009.
[6] A. Woolfitt *et al.*, "Quantitative mass spectrometry for bacterial protein toxins—A sensitive, specific, high-throughput tool for detection and diagnosis," *Molecules*, vol. 16, no. 3, pp. 2391–2413, 2011.
[7] D. R. Franz *et al.*, "Clinical recognition and management of patients exposed to biological warfare agents," *JAMA*, vol. 278, pp. 399–411, Aug. 1997.
[8] J. B. Tucker, *Toxic Terror: Assessing Terrorist Use of Chemical and Biological Weapons*. Cambridge, MA, USA: MIT Press, 2000.

[9] S. WuDunn, J. Miller, and W. J. Broad, "How Japan germ terror alerted world," *New York Times*, vol. 26, pp. A1–A10, May 1998.

[10] S. S. Arnon *et al.*, "Botulinum toxin as a biological weapon: Medical and public health management," *JAMA*, vol. 8, pp. 1059–1070, Feb. 2001.

[11] E. Aranda, M. M. Rodriguez, M. A. Asensio, and J. J. Cordoba, "Detection of clostridium botulinum types A, B, E and F in foods by PCR and DNA probe," *Lett. Appl. Microbiol.*, vol. 25, no. 3, pp. 186–190, 1997.

[12] F. Anniballi, B. Auricchio, E. Delibato, M. Antonacci, D. Medici, and L. Fenicia, "Multiplex real-time PCR SYBR Green for detection and typing of group III *Clostridium botulinum*," *Vet. Microbiol.*, vol. 154, pp. 332–338, Jan. 2012.

[13] M. Lindstrom and H. Korkeala, "Laboratory diagnostics of botulism," *Clin. Microbiol. Rev.*, vol. 19, no. 2, pp. 314–398, 2006.

[14] L. M. Wein and Y. Liu, "Analyzing a bioterror attack on the food supply: The case of botulinum toxin in milk," *Proc. Nat. Sci. USA*, vol. 102, no. 28, pp. 9984–9989, Jul. 2005.

[15] G. Deng and G. Sanyal, "Applications of mass spectrometry in early stages of target based drug discovery," *J. Pharmaceutical Biomed. Anal.*, vol. 40, no. 3, pp. 528–538, Feb. 2006.

[16] T. Grenda, E. Kukier, and K. Kwiatek, "Methods and difficulties in detection of Clostridium botulinum and its toxins," *Polish J. Vet. Sci.*, vol. 17, no. 1, pp. 195–205, 2014.

[17] S. S. Sridharamurthy, A. K. Agarwal, D. J. Beebe, and H. Jiang, "Dissolvable membranes as sensing elements for microfluidics based biological/chemical sensors," *Lab Chip*, vol. 6, no. 7, pp. 840–842, May 2006.

[18] M. L. Frisk, W. H. Tepp, G. Lin, E. A. Johnson, and D. J. Beebe, "Substrate-modified hydrogels for autonomous sensing of botulinum neurotoxin type A," *Chem. Mater.*, vol. 44, no. 19, pp. 5842–5844, 2007.

[19] X. Wu *et al.*, "Microfluidic detection of botulinum neurotoxin type a utilizing polyacrylamide hydrogels with SNAP-25 peptide crosslinker," *IEEE Sensors J.*, vol. 15, no. 2, pp. 1091–1097, Feb. 2015.

[20] X. Wu *et al.*, "A microfluidic sensor of botulinum neurotoxin type a utilizing SNAP-25 incorporated responsive hydrogel," in *Proc. IEEE Sensors*, Baltimore, MD, USA, Nov. 2013, pp. 629–632.

[21] R. V. Ulijin *et al.*, "Bioresponsive hydrogels," *Mater. Today*, vol. 10, no. 4, pp. 40–48, 2007.

[22] A. Mateescu, Y. Wang, J. Dostalek, and U. Jonas, "Thin hydrogel films for optical biosensor applications," *Membranes*, vol. 2, no. 1, pp. 40–69, 2012.

[23] R. Wolthuis, D. McCrae, E. Saaski, J. Hartl, and G. Mitchell, "Development of a medical fiber-optic pH sensor based on optical absorption," *IEEE Trans. Biomed. Eng.*, vol. 39, no. 5, pp. 531–537, May 1992.

[24] S. Tierneya, S. Voldenb, and B. T. Stokkea, "Glucose sensors based on a responsive gel incorporated as a Fabry–Perot cavity on a fiber-optic readout platform," *Biosensors Bioelectron.*, vol. 24, no. 7, pp. 2034–2039, 2009.

[25] N. Massad-Ivanir, G. Shtenberg, T. Zeidman, and E. Segal, "Construction and characterization of porous SiO_2/hydrogel hybrids as optical biosensors for rapid detection of bacteria," *Adv. Funct. Mater.*, vol. 20, no. 14, pp. 2269–2277, 2010.

[26] D. R. Hjelme, O. Aune, B. Falch, D. Østling, and R. Ellingsen, "Fiber-optic biosensor technology for rapid, accurate and specific detection of enzymes," in *Proc. Opt. Sensors Conf.*, Barcelona, Spain, Jul. 2014, pp. 27–31.

[27] C.-H. Lin, L. Jiang, H. Xiao, Y.-H. Chai, S.-J. Chen, and H.-L. Tsai, "Fabry–Perot interferometer embedded in a glass chip fabricated by femtosecond laser," *Opt. Lett.*, vol. 34, no. 16, pp. 2408–2410, Aug. 2009.

[28] J. Villatoro, V. Finazzi, G. Coviello, and V. Pruneri, "Photonic-crystal-fiber-enabled micro-Fabry–Perot interferometer," *Opt. Lett.*, vol. 34, no. 16, pp. 2441–2443, 2009.

[29] B. Schyrr, S. Boder-Pasche, R. Ischer, R. Smajda, and G. Voirin, "Fiber-optic protease sensor based on the degradation of thin gelatin films," *Sens. Bio-Sens. Res.*, vol. 3, pp. 65–73, Mar. 2002.

[30] B. Qi *et al.*, "Novel data processing techniques for dispersive white light interferometer," *Opt. Eng.*, vol. 42, no. 11, pp. 3165–3171, 2003.

[31] D. A. Benaron and K. Stevenson, "Optical time-of-flight and absorbance imaging of biologic media," *Science*, vol. 259, pp. 1463–1466, Mar. 1993.

Xiudong Wu received the B.S. degree from the Beijing Institute of Petrochemical Technology, Beijing, China, in 2006, the M.S. degree in electrical engineering from Peking University, Beijing, in 2011, and the Ph.D. degree in electrical engineering from the University of Wisconsin–Madison, Madison, WI, USA, in 2017. His research interests include toxin detection in food, microelectronic, and microelectromechanical systems fabrication process.

Hewei Liu received the B.S. and Ph.D. degrees from Xi'an Jiaotong University, China, in 2006 and 2012, respectively. He is currently an Assistance Scientist with the Department of Electrical and Computer Engineering, University of Wisconsin–Madison. His research interests include optical sensors, bioinspiration devices, and micro-/nano-manufacturing technologies.

Xiaodong Wang received the B.S. degree in optoelectronics science and technology from Nankai University, Tianjin, China, in 2011, and the M.S. degree in electrical engineering from the University of Wisconsin–Madison in 2013. He is currently pursuing the Ph.D. degree in electrical engineering. His research interests include semiconductor laser device simulation and fabrication, microwave mode converter design, and Gaussian beam diffraction grating design.

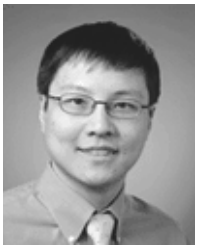

Hongrui Jiang (S'98–M'02–SM'10–F'17) received the B.S. degree in physics from Peking University, Beijing, China, and the M.S. and Ph.D. degrees in electrical engineering from Cornell University, Ithaca, NY, USA, in 1999 and 2001, respectively. From 2001 to 2002, he was a Post-Doctoral Researcher with the Berkeley Sensor and Actuator Center, University of California at Berkeley. He is currently the Vilas Distinguished Achievement Professor and the Lynn H. Matthias Professor of Engineering with the Department of Electrical and Computer Engineering, a Faculty Affiliate with the Department of Biomedical Engineering, the Department of Materials Science and Engineering, and the Department of Ophthalmology and Visual Sciences, and a member of the McPherson Eye Research Institute with the University of Wisconsin–Madison. His research interests are in microfabrication technology, biological and chemical microsensors, microactuators, optical microelectromechanical systems, smart materials and micro-/nanostructures, lab-on-chip, and biomimetics and bioinspiration.

Dr. Jiang is a Fellow of the Institute of Physics, the Royal Society of Chemistry, the American Institute for Medical and Biological Engineering, and the Institute of Institute of Electrical and Electronics Engineers. He was a recipient of the National Science Foundation CAREER Award and the Defense Advanced Research Projects Agency Young Faculty Award in 2008, the H. I. Romnes Faculty Fellowship of the University of Wisconsin–Madison in 2011, the National Institutes of Health Director's New Innovator Award in 2011, the Vilas Associate Award of the University of Wisconsin in 2013, and the Research to Prevent Blindness Stein Innovation Award in 2016. He is a member of the Editorial Board of the IEEE/ASME JOURNAL OF MICROELECTROMECHANICAL SYSTEMS.